

Bomin Sun\*, Lisan Yu, and Robert A. Weller

Department of Physical Oceanography, Woods Hole Oceanographic Institution, Woods Hole, MA

## 1. INTRODUCTION

Accurate basin-scale air-sea heat fluxes are needed to better understand and predict climate variability and change. Numerical Weather Prediction (NWP) analysis-forecast systems, e.g., the National Center for Environmental Prediction Reanalyses 1 and 2 (NCEP1 and NCEP2) and the European Centre for Medium Range Weather Forecasting (ECMWF), provide 6-hourly fluxes with global coverage. However, data-model comparative studies carried out in regions of the world's oceans (i.e., Weller and Anderson 1996; Wang and McPhaden 2001) indicate that the ocean turbulent heat losses in NWP models are overestimated. Sun et al. (2001) compared the NWP model analyses with moored buoy observations in the Atlantic and found that the overestimation in time-mean latent heat loss ranges from about  $14 \text{ W m}^{-2}$  (13%) in the eastern subtropical North Atlantic to about  $29 \text{ W m}^{-2}$  (30%) in the tropics and to about  $30 \text{ W m}^{-2}$  (49%) in the midlatitude coastal area, where the overestimation in sensible heat flux reaches about  $20 \text{ W m}^{-2}$  (60%). These systematic overestimations result primarily from the biases in bulk variables and the use of inappropriate bulk aerodynamic formulas. The contributions of these two factors to the heat flux biases vary with region and NWP model.

This study describes the methodology to produce an improved daily gridded surface turbulent heat flux product in the Atlantic basin for 1988-1999. We use an advanced objective analysis technique to optimize the individual bulk variables through synthesizing data from NWP model analyses and satellite measurements. The state-of -the-art TOGA COARE flux algorithm 2.6 version (Bradley et al. 2001) is applied to those optimized variables, thus to develop the surface latent and sensible heat fluxes. The technique we use is based on a variational approach (Legler et al. 1989; Jones et al. 1995; Yu et al. 2001). The approach combines fields in a nonlinear least squares format and the solution is the field that best minimizes a functional that expresses several constraints or "lack of fit" operating on observations, background fields, and other physical and dynamical expectations. For this analysis, the functional includes weighted misfit constraints for NCEP2, ECMWF, and satellite measurements along with time evolution and Laplacian constraints that are intended to smooth solution fields. Each constraint of the functional is weighted based primarily on existing knowledge of the

regional strengths and weaknesses of each dataset, which is briefly described in the next section.

## 2. DATA

The bulk variables used to calculate air-sea turbulent heat fluxes include wind speed, air temperature and humidity, and sea surface temperature. Daily data of these variables from the NCEP2 reanalysis and the operational ECMWF analysis, and daily sea surface temperature from the Advanced Very High Resolution Radiometer (AVHRR) and the Special Sensor Microwave Imager (SSM/I)-derived 10-m wind speed and humidity are used as input datasets in the direct minimization approach. All the datasets cover the period of 1988-1999 except the SSM/I humidity data, which last from 1988 to 1994. These datasets are compared to each other and also to moored buoy measurements in regions of the Atlantic, including the eastern subtropical North Atlantic, the tropical Atlantic and the western coast of the North Atlantic (Figure 1). The SSM/I 10-m humidity is height-adjusted to 2-m humidity using the COARE2.6a flux algorithm in order to be comparable with NWP and buoy 2-m humidity data. The details of the comparison for NWP versus buoy data are described in Sun et al. (2001). The following is a summary of this comparison.

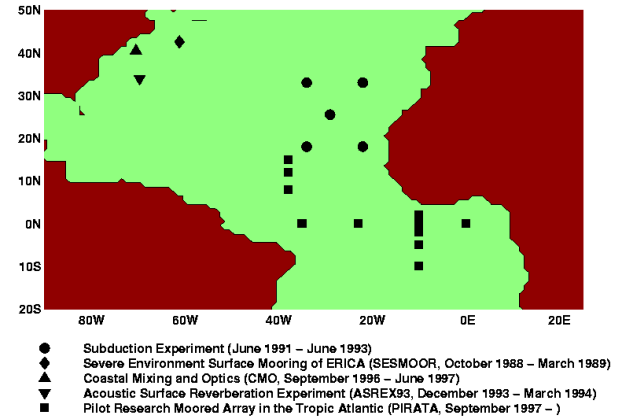


Figure 1. Locations of moored buoys used for comparison with NWP and satellite data.

The 10-m wind speeds from NCEP2 and particularly from ECMWF are weaker. In the tropics, the NCEP2 and ECMWF wind speeds show low biases of  $0.4 \pm 1.2 \text{ m s}^{-1}$  and  $0.7 \pm 0.8 \text{ m s}^{-1}$  respectively. The SSM/I-derived wind speeds are higher than ECMWF and NCEP2 by about  $0.6 \text{ m s}^{-1}$  and  $1.0 \text{ m s}^{-1}$  in the northern tropical and subtropical regions, and are closer to NCEP2 in other regions. The 2-m humidity from

\*Corresponding author address: Bomin Sun, Department of Physical Oceanography, Woods Hole Oceanographic Institution, Woods Hole, MA 02543, e-mail: bsun@whoi.edu

NCEP2 and particularly ECMWF is close to buoy data in the extratropical region while dry biases of  $0.3 \pm 0.7 \text{ g kg}^{-1}$  and  $1.0 \pm 0.6 \text{ g kg}^{-1}$  in the low latitude are shown in NCEP2 and in ECMWF respectively. The SSM/I 2-m humidity shows a humid bias in the low latitude. The 2-m temperature and sea surface temperature from NCEP2 and ECMWF basically are close to buoy data except in the west coastal region, where significant biases are found in NWP. Compared to NWP, the sea surface temperatures from AVHRR generally are slightly lower in the northern tropics and higher in the other regions.

The temporal variability comparison indicates that the NWP sea surface temperatures are poorly represented on short-time scales. On daily basis, the variability of bulk variables from NWP models generally are not represented well except in the coastal region, where the NWP systems assimilated large quantities of in-situ data. NCEP2 and ECMWF show a similarity in temporal variability except the variability in sea surface temperature, which differs between them and also differs from buoy data.

The above information is used in this analysis to subjectively determine the relative weighting of each misfit term in the cost functional. The following section describes the details of the functional, its minimization, and the sensitivity analysis performed to determine the response of solution fields to weights for each of the terms.

### 3. METHODOLOGY

In this analysis, the desired products for 2-m air temperature and surface pressure are synthesized from NCEP2 and ECMWF datasets only and for 10-m wind speed, 2-m humidity and sea surface temperature, are synthesized from NCEP2, ECMWF and satellite measurements. The functional to be minimized,  $F$ , is designed to combine the two/three datasets into a field. The general formula of functional  $F$  can be written as

$$F = \alpha \sum R_n (X - X_{ncep2})^2 + \beta \sum R_e (X - X_{ecmwf})^2 + \gamma \sum R_s (X - X_{satellite})^2 + \delta \sum (\Delta X / \Delta t)^2 + \epsilon L^2 \sum (\nabla^2 (X - X_{ncep2}))^2 \quad (1)$$

The first three terms of  $F$  represent the misfit of the NCEP2, ECMWF, and satellite (for 10-m wind speed, 2-m humidity and sea surface temperature only) fields with respect to the solution field. The forth term is the time evolution and the fifth term is the Laplacian or smoothing term.

$R_n$ ,  $R_e$ , and  $R_s$  are the inversions of the error variance of NCEP2, ECMWF and satellite data respectively, and  $\alpha$ ,  $\beta$ ,  $\gamma$ ,  $\delta$ ,  $\epsilon$  are subjectively determined constants.  $L$  is the length of one grid spacing, approximately 110 km. The error variances  $R_n$ ,  $R_e$ , and  $R_s$  are determined from monthly NCEP2, ECMWF and satellite data against the Southampton Oceanography Centre (SOC) global air-sea heat flux analysis data (Josey et al. 1998). The monthly SOC analysis was generated from the Comprehensive Ocean-Atmosphere Data Set (COADS) Volunteer Observing Ship reports and is available from 1980-

1997. The systematic error arising from variations in observing procedure for each individual ship meteorological report has been corrected. Validation studies indicate that SOC climatology are generally in good agreement with buoy measurements. In this analysis, SOC data are thus regarded as the "truth" data to obtain the spatial error variance of the NWP and satellite data. In the next section, SOC fluxes are also used as one of the reference datasets to validate our synthesis fluxes. The basin-scale patterns of  $R_n$ ,  $R_e$ , and  $R_s$  are basically similar to each other. For example, large variances of bulk variables from NWP and satellite data are generally found in the northern high latitudes and southern extratropical regions, where VOS ship data are sparse and NWP analyses are less reliable.

Some criteria are used to determine the optimal weights of  $\alpha$ ,  $\beta$ ,  $\gamma$ ,  $\delta$ ,  $\epsilon$ , including sufficient weightings to retain the basin-scale pattern exhibited in NWP data, the quality of the input datasets as determined through comparisons to buoy data, and finally the sensitivity experiments. The values of the time evolution and spatial smoothing weights  $\delta$ ,  $\epsilon$  are uniform for all grid points within the analysis domain. These weights are smaller in magnitude than  $\alpha$ ,  $\beta$  or  $\gamma$  in order not to distort the realistic temporal-spatial patterns of the bulk variables.

In order to possibly account for the systematic errors of the input datasets in the direct minimization, we determine the values of  $\alpha$ ,  $\beta$ ,  $\gamma$ , in such a way that their individual products with the inversions of their corresponding datasets' basin-averaged error variance (calculated from  $R_n$ ,  $R_e$ , and  $R_s$  respectively) are proportional to the relative strengths of those datasets as described in section 2. For example, the averaged 10-m wind speed error variances for NCEP2, ECMWF and SSM/I are 0.59, 0.64 and 0.91 respectively. We therefore assign 20, 10 and 40 to  $\alpha$ ,  $\beta$  and  $\gamma$ , implying that on basin-scale the ECMWF winds have errors about 2 times larger than NCEP2 and 2.6 times larger than SSM/I. In other words, the values of the weights  $R_n$ ,  $R_e$ , and  $R_s$  are expected to lead to the SSM/I data contribution to the solution about the same as the sum of the contributions of NCEP and ECMWF data.

The weights in Equation 1 are subjectively determined that can have a significant impact on the solution fields. Analysis of the sensitivity of the weights, that is, the change in the solution per change in the weight, provides hints in selecting suitable values. Sensitivity tests are therefore performed on each of the weights in the functional to understand the effects on the solution fields. Our survey indicates that generally there is a less than 1% change in solution fields for a 10% change in our prescribed weights. The 10-m wind speed sensitivity test is shown next as an example.

Figure 2 indicates that for a 50% increase in the weight of the SSM/I wind speed term, the solution linearly increases with the wind speed difference of the SSM/I and NWP. For a wind speed difference of 30% (98% of the grid points are within this value), the solution increases with the SSM/I weight (Figure 3). However, the weight increase becomes larger when the solution increase becomes smaller. The change in

solution is quite small as response to the change in weight. As shown in Figure 3, for a presumed uncertainty of 100% in the weight, the “error” of the result reaches only 4%, about  $0.4 \text{ m s}^{-1}$  with monthly wind speed of  $10 \text{ m s}^{-1}$ . These experiments indicate that the synthesized result is stable and our prescribed weights are acceptable.

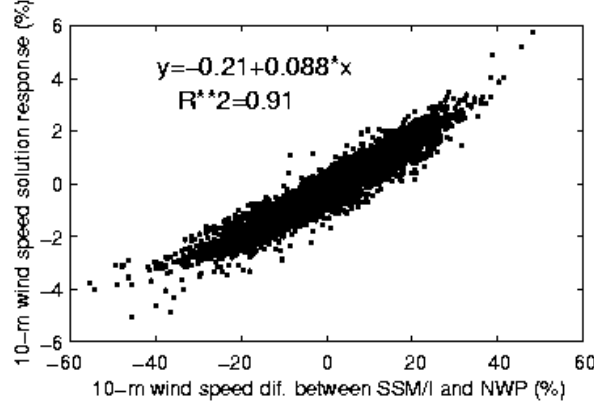


Figure 2. Relationship between the response of the 10-m wind speed solution to the wind speed difference between SSM/I and NWP for the case of the SSM/I term weight increasing by 50%. Each dot represents a grid point in the Atlantic basin for January 1992.

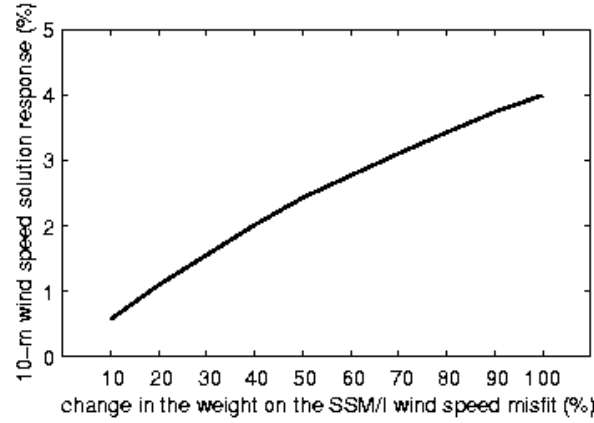
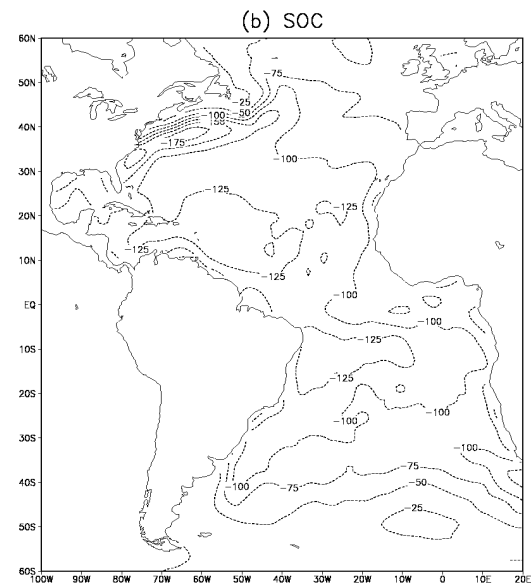
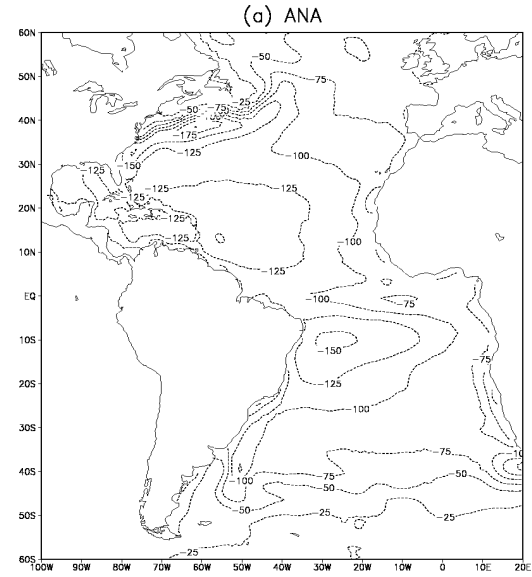


Figure 3. Response of the 10-m wind speed solution to the change in the SSM/I weight for the case of the wind speed difference between SSM/I and NWP equal to 30%.

#### 4. RESULTS

Using the technique described previously, daily fields of each of the 5 bulk variables at  $1 \times 1$  grid are produced for the period 1988-1999. Daily surface latent and sensible heat fluxes are then estimated using the COARE2.6a flux algorithm. Here we focus on air-sea latent flux results.



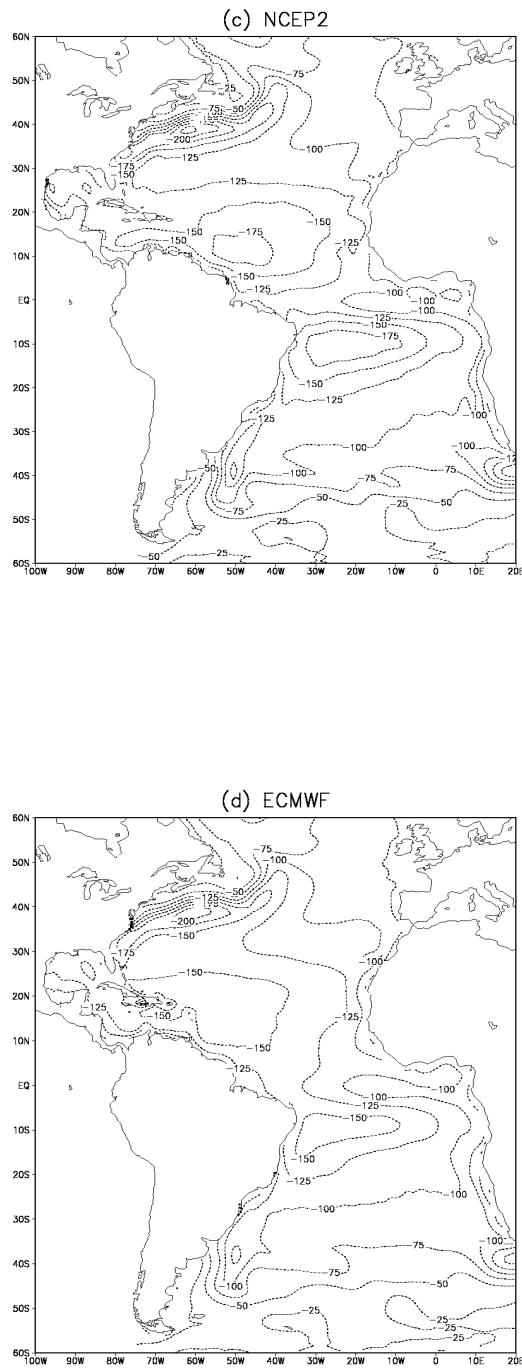


Figure 4. Annual mean latent heat flux ( $\text{W m}^{-2}$ ) for 1988-1997 for our analysis result (a) in comparison with SOC (b), NCEP2 (c) and ECMWF (d)

The basin-scale pattern shown in our analysis (Figure 4 (a)) is similar to those in SOC, NCEP2 and

ECMWF. All the datasets demonstrate larger oceanic latent heat loss in the gulf stream and the subtropical trade belts. However, the NWP models show latent heat loss much larger than our analysis and SOC. the climatological latent heat loss in our analysis is very similar on basin-scale to SOC, which is likely to be reliable (Josey et al. 1999).

Moored buoy data sparsely distributed in the Atlantic (Figure 1) are not synthesized in this analysis, and hence, are qualified to be used as the independent “ground truth” reference datasets for the validation. These buoy data are collected from deployments in different time periods of 1988-1999 .

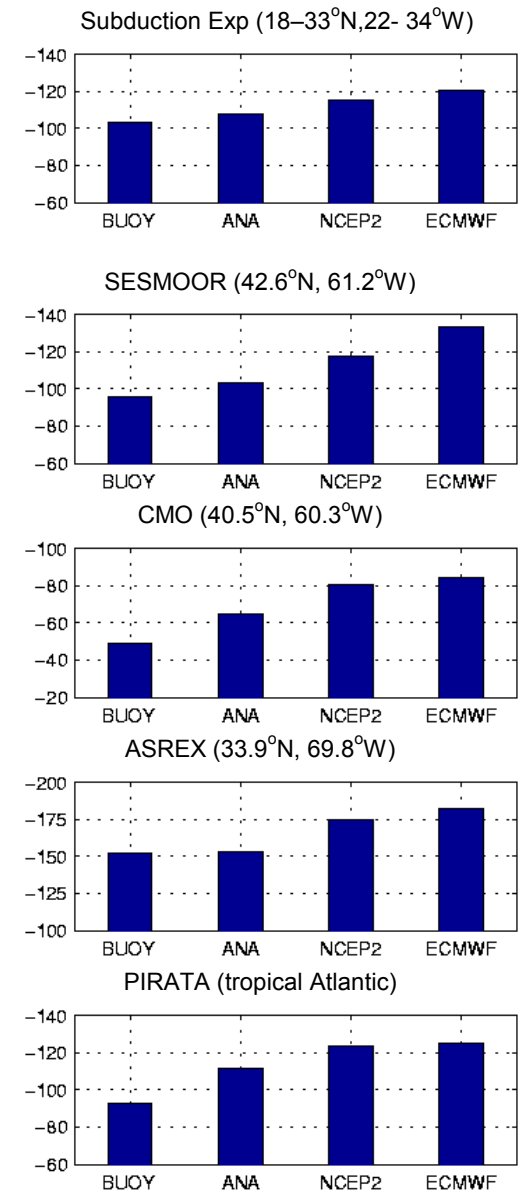


Figure 5. Comparison of buoy latent flux with flux from our analysis, NCEP2 and ECMWF at buoy sites shown in Figure 1. Unit:  $\text{W m}^{-2}$ .

In all the buoy experiments considered, our flux product is much closer to buoy measurements than NCEP2 or ECMWF. The NWP models are again seen to overestimate latent heat loss as we notice from the basin-scale comparison (Figure 4). It is noted from Figure 5 that our analysis has a larger deviation at the PIRATA buoy sites, which partly results from that fact that the 2-m humidity analysis (1995-1999) came from the dry-biased NCEP2 and ECMWF (in the tropics). (The PIRATA experiment started in 1998. The SSM/I-derived humidity is available for 1988-1994 and is higher than the NWP humidity in the tropics).

The improvement of our synthesis heat flux product over the NWP as described in Figures 4 and 5 come from the less biased synthesis bulk variables and the use of the COARE2.6a algorithm (Zeng et al. 1998). At the buoy reference sites (Figure 1) where a strict validation can be conducted, the synthesized bulk variables particularly the 10-m wind speed and 2-m humidity are found to become more accurate in time-mean values and their daily mean rms differences from buoy data become smaller than the NWP counterparts.

## 5. SUMMARY

Daily surface turbulent heat fluxes in the Atlantic for 1988-1999 are produced by applying the COARE2.6a flux algorithm to the bulk variables synthesized from NWP models and satellite measurements using the variational-direction minimization approach. The optimal weights in this objective analysis technique were selected based on existing knowledge of the strengths/weaknesses of the input datasets through comparing with in-situ data and on weight sensitivity tests. The validation with ship and buoy data indicates that the heat fluxes from our analysis shows significant improvement over the NWP fluxes.

## 6. REFERENCES

Bradley, E.F., C.W. Fairall, J.E. Hare, and A.A. Grachev, 2000: An old and improved bulk algorithm for air-sea fluxes: COARE2.6A, AMS Symposium on Turbulence and Boundary Layers, Snowmass, Utah.

Jones, C.S., D.M. Legler, and J.J. O'Brien, 1995: Variability of surface fluxes over the Indian Ocean: 1960-1989. *The Global Atmosphere and Ocean System*, Amsterdam B.V. Published in the Netherlands, Vol.3, pp. 249-272

Josey, S.A., E.C. Kent, and P.K. Taylor, 1998: *The Southampton Oceanography Centre (SOC) Ocean-Atmosphere Heat, Momentum and Freshwater Flux Atlas*. Report No. 6, Southampton Oceanography Centre, Southampton, UK, 30pp+figs.

Josey, S.A., E.C. Kent, and P.K. Taylor, 1998: New insights into the ocean heatbudget closure problem from analysis of the SOC air-sea flux climatology. *J. Climate*, **12**, 2856-2880.

Legler, D.M., I.M. Navon, and J.J. O'Brien, 1989: Objective analysis of pseudostress over the Indian Ocean using a direct-minimization approach. *Mon. Wea. Rev.*, **117**, 709-720.

Sun, B., L. Yu, and R.A. Weller, 2001: Comparisons of surface meteorology and turbulent heat flux over the Atlantic: NWP model analyses versus moored buoy observations. *J. Climate* (submitted).

Wang, W., and M.J. McPhaden, 2001: What is the mean seasonal cycle of surface heat flux in the equatorial Pacific? *J. Geophys. Res.*, **106**, 837-857.

Weller, R.A., and S.P. Anderson, 1996: Surface meteorology and air-sea fluxes in the western equatorial Pacific Warm Pool during the TOGA Coupled Ocean-Atmosphere Response Experiment. *J. Climate*, **9**, 1959-1990.

Yu, L., B. Sun, and R.A. Weller, 2001: New daily air-sea flux fields for the Atlantic Ocean -preliminary results. *Proceeding of the WCRP/SCOR workshop on Intercomparison and Validation of Ocean-Atmosphere Flux Fields*, Potomac, Maryland, May 21 – May 24, 2001.

Zeng, X., M. Zhao, and R.E. Dickinson, 1998: Intercomparison of bulk aerodynamic algorithms for the computation of sea surface fluxes using TOGA COARE and TAO data. *J. Climate*, **11**, 2628-2644.

## ACKNOWLEDGEMENTS

This work is supported by the NOAA CLIVAR-Atlantic program under Grant NA06GP0453. The authors gratefully acknowledge Simon Josey at the Southampton Oceanography Centre, Southampton, UK for providing the SOC flux dataset.